Phys. Status Solidi RRL 6, No. 5, 199–201 (2012) / DOI 10.1002/pssr.201206099

pss +++rapid research letters+++
www.pss-rapid.com

Plasmon enhanced light absorption in bulk heterojunction organic solar cells

Xiaohan Yang*, Ashraf Uddin, and Matthew Wright

School of Photovoltaic and Renewable Energy Engineering, University of New South Wales, 2052 Sydney, Australia

Received 9 March 2012, revised 12 April 2012, accepted 12 April 2012
Published online 16 April 2012

Keywords Ag nanospheres, light absorption, P3HT:PCBM, surface plasmons

* Corresponding author: e-mail xiaohan.yang@unsw.edu.au, Phone: +61 2 9385 9827, Fax: +61 2 9385 5104

Silver nanospheres (Ag NSs) buffer layers were introduced via a solution casting process to enhance the light absorption in poly (3-hexylthiophene) (P3HT) and [6,6]-phenyl-C61 butyric acid methyl ester (PCBM) bulk heterojunction organic solar cells. These Ag NSs, as surface plasmons, could increase the optical electric field in the photoactive layer whilst simultaneously improving the light scattering. As a result, this buffer layer improves the light absorption of P3HT:PCBM blend and consequently improves the external quantum efficiency (EQE) of organic solar cells. In this work, different sizes of Ag NSs plasmon-enhanced layer were investigated, with the aim of optimizing the performance of devices. UV-vis spectrometer measurement demonstrates that the total optical absorption of P3HT:PCBM blend films in the spectral range of 350–650 nm is increased by ~4 and 6% with incorporation of the 20 and 40 nm Ag NSs, respectively. The J_{sc} was shown to increase by ~21 and 24% for 20 and 40 nm Ag NSs, respectively. This is due to the extra photogenerated excitons by the plasmonic resonance of Ag NSs.

1 Introduction Organic photovoltaic (OPV) devices have attracted much attention in recent years due to the associated potential benefits that the technology may yield. In particular, low-cost production methods, mechanically flexible substrates and very thin active layer films, due to the excellent absorption properties of the organic materials, may lead to very low cost photovoltaic devices [1]. To date, the highest reported power conversion efficiency (PCE) for an OPV device is 10% [2], which is approaching what is deemed to be required for commercialization. However, the most commonly studied polymer–fullerene system is based on P3HT:PCBM, for which the highest reported PCE values are in the range of 4.5% to 6% [3, 4].

Due to the small physical dimensions of the photoactive layer, the ability to absorb a large fraction of the solar spectrum is a crucial parameter in determining the efficiency of OPV devices. Several approaches have been investigated to maximize the absorption of the photoactive layer. These include the usage of low-bandgap polymers that absorb the red and near-infrared parts of the solar spectrum [5], the implementation of an inorganic optical spacer between the active layer and metal electrode [6], and the incorporation of metal nanostructures to increase the absorption of organic materials due to the high electric field provided by the excited surface plasmons [7]. Plasmonic materials have also been utilized in semiconductor devices including light-emitting diodes, silicon photodiodes, electrochromic devices and solar cells [8]. These materials are advantageous due to the large electromagnetic field enhancement near the metal surface and strong dependence of the resonance wavelength on size, shape, and local dielectric environment of the metal nanostructures [9]. Recently, Fung et al. [10] have investigated the influence of Au nanoparticles (NP) concentration on the plasmonic enhancement of PCE for P3HT:PCBM solar cells, however, the size of the Au NPs was kept constant at ~18 nm.

In this Letter, plasmonic enhancement of the P3HT:PCBM bulk heterojunction system is demonstrated in a spin-cast device with an incorporated thin Ag film. Such films consist of plasmon-active and size-variable Ag NSs. Incorporation of a plasmon-active material is shown to enhance absorbance of photoactive layer. Consequently, enhancements of EQE at red wavelengths were observed.

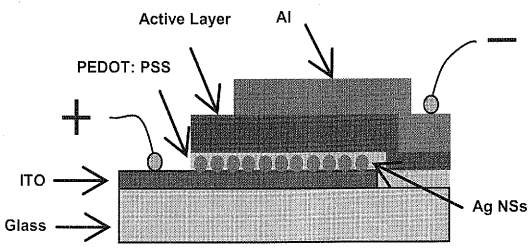

Figure 1 (online colour at: www.pss-rapid.com) Schematic diagram of organic solar cell device structure. The ITO and Al layers were used as anode and cathode, respectively.

2 Experimental Highly pure P3HT (99.995%), PCBM (99%), poly(3,4-ethylenedioxythiophene)-poly (styrenesulfonate) (PEDOT:PSS) and 1,2-dichlorobenzene were purchased from Sigma-Aldrich for this study. 20 nm and 40 nm Ag NSs (0.02 mg/mL in aqueous citrate) were purchased from nanoComposix. Regioregular P3HT was blended with PCBM and then dissolved in 1,2-dichlorobenzene to produce a P3HT:PCBM (20:20 mg/mL) solution. This solution was then stirred with a magnetic stirrer on a hotplate for 3 h at 70 °C. After stirring, the solution was filtered using a 0.45 μm PTFE syringe filter. The device structure used was ITO/Ag NSs/PEDOT:PSS/P3HT:PCBM/Al, as shown in Fig. 1.

The ITO glass substrates (50 × 50 mm) were ultrasonicated in deionized (DI) water, acetone and isopropyl alcohol, each for 10 min. Subsequently, an Ag NSs buffer layer was spin coated on the ITO substrate at 2000 rpm. Then, a layer of the hole-conductive polymer PEDOT:PSS was spin coated on the top of Ag NSs film to form a thin film of about 50 nm thickness, as measured by a Bruker optical profilometer. This substrate was then dried at 100 °C in an oven for 10 min to remove the water. Next, a 120 nm thick P3HT:PCBM active layer was deposited by spin coating. P3HT:PCBM blend films were placed in a Petri dish for storage in a nitrogen atmosphere. Device fabrication was completed by the thermal evaporation of a 100 nm thick aluminum (Al) layer at a background pressure of 10^{-5} Torr. Each substrate was prepared with 6 identical samples. Finally, devices were thermally annealed at 130 °C for 20 min in a nitrogen atmosphere. Three types of solar cells (with only PEDOT:PSS, with 20 nm Ag NSs/PEDOT:PSS and with 40 nm Ag NSs/PEDOT:PSS in the buffer layer) were made for comparison in this experiment. All the transmission electron microscopy (TEM), UV–vis absorbance spectra and EQE measurements were performed in air on non-encapsulated devices at room temperature. TEM images were taken on a JEOL 1010 transmission electron microscope. Absorbance was measured using a Perkin–Elmer UV–vis spectrometer (Lambda 1050). EQE data was measured with a QEX10 quantum efficiency measurement system from PV Measurements, Inc. All measurements were performed within two days of device fabrication. The samples were stored in a nitrogen desiccator to minimize the effects of oxidation.

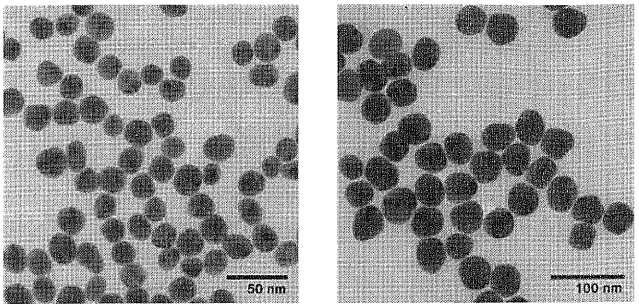

Figure 2 (online colour at: www.pss-rapid.com) TEM images of 20 nm (left) and 40 nm (right) of Ag NSs in solutions.

3 Results and discussion Figure 2 shows TEM images of purchased Ag NSs in solutions. As shown, Ag NSs are all spherical in shape and highly monodispersed, and have average diameters of (a) 20 nm and (b) 40 nm, respectively.

Figure 3 shows the UV–vis absorbance spectrum of P3HT:PCBM blend films with and without Ag NSs buffer layer. For the control blend, with no buffer layer (black dashed line), two main absorption peaks at ~350 nm and 510 nm are observed, which correspond to PCBM and P3HT, respectively. Absorption in the blend film is contributed to primarily by P3HT. It has a higher magnitude of absorbance compared to PCBM, in the spectral range of 450 nm to 600 nm. The presence of a vibronic structure in regioregular P3HT is observed at ~600 nm. This vibronic structure is due to the ordered state achieved by the regioregular P3HT [11]. Incorporation of the Ag NSs buffer layers slightly enhances the absorbance spectra. The total optical absorption of P3HT:PCBM blend films in the spectral range of 350–650 nm is increased ~4% and 6% as a result of incorporation of the 20 nm and 40 nm Ag NSs,

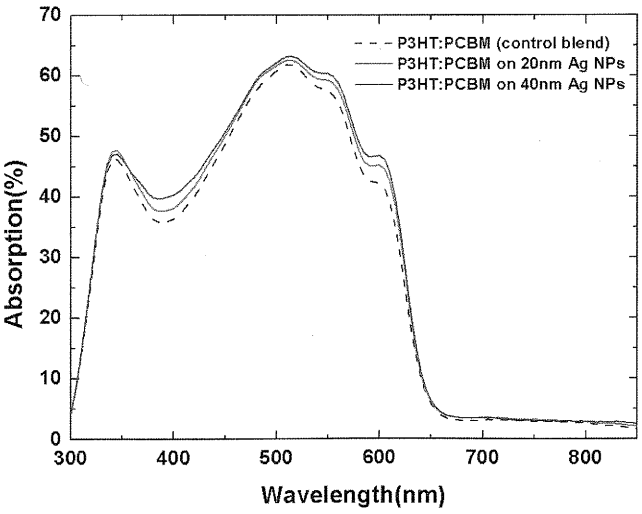

Figure 3 (online colour at: www.pss-rapid.com) Optical absorbance spectra of P3HT:PCBM blend films with Ag NSs 20 nm (red solid), 40 nm (blue solid), and control blend (black dashed line).

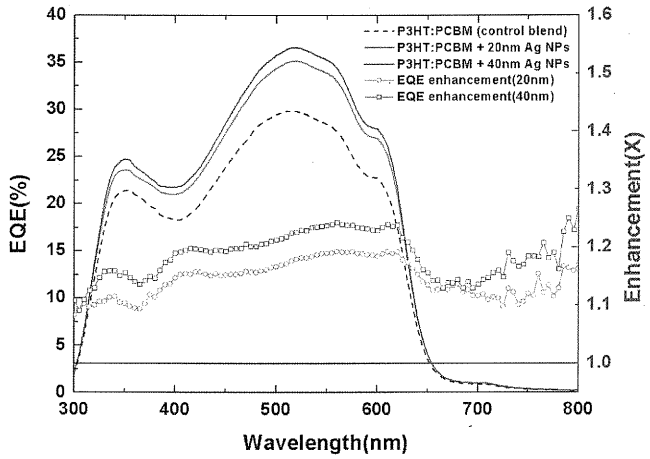

Figure 4 (online colour at: www.pss-rapid.com) EQE spectra of P3HT:PCBM devices with Ag NSs 20 nm (red solid line), 40 nm (blue solid line), and control blend (black dashed line) (left-hand axis). Enhancements of EQE for the devices with 20 nm (red circles) and 40 nm (blue squares) size Ag NSs buffer layer (right-hand axis).

respectively. This is attributed to light scattering of the Ag NSs and the increased electric field in the photoactive layer by excited localized surface plasmons around the Ag NSs [12].

Figure 4 displays the EQE spectra of P3HT:PCBM devices with and without Ag NSs buffer layer. The secondary axis displays the enhancements in EQE, due to the addition of a Ag NS buffer layer. This is a unitless multiplication factor. Although our OPV devices have not been optimized, significant changes in electrical performance as a result of localized surface plasmonic resonance have been observed. The EQE profile of the control device (black dashed line) primarily follows the profile of optical absorbance of the P3HT:PCBM blend film, and has a maximum EQE value of ~29.9% at 510 nm. With the presence of a Ag NSs buffer layer, the maximum EQE values are increased to ~35.2 and 36.6% at 520 nm for 20 nm and 40 nm Ag NSs, respectively. The calculated maximum enhancements in the spectral range 300–650 nm are 1.19 and 1.24 for 20 nm and 40 nm Ag NSs, respectively. By integrating the products of this EQE and the global reference solar spectrum, the short-circuit current densities (J_{sc}) were calculated to be ~3.93 mA/cm^2 for the control device, ~4.76 mA/cm^2 and 4.89 mA/cm^2 for 20 nm and 40 nm Ag NSs, respectively. This represents an increase of ~21% and 24% for 20 nm and 40 nm Ag NSs, with reference to the control device. The larger-sized Ag NSs led to a larger enhancement of J_{sc}, which is thought to result from enhanced scattering interactions. With the incorporation of Ag NSs, an additional photocurrent is created due to the enhancement of the photogeneration of excitons associated with an enhanced electric field intensity from the localized surface plasmonic resonance. This plasmonic coupling of light is a major contributor to the improved electronic transport through the blend films.

The placement of the Ag NSs buffer layer is crucial in determining its impact on the device. There exists a trade-off related to the distance between the buffer layer and the photoactive layer. Placing the buffer layer in contact with the photoactive layer can significantly increase the surface recombination [13], and thus, there should be some physical separation between the two. However, the electric field caused by the excited surface plasmons decays exponentially with distance from the layer [14]. This implies that there is some nonobvious physical separation required, between the Ag NS buffer layer and the photoactive layer of the device, which will allow for the maximum improvement to be obtained. Further optimization of the plasmon enhanced organic bulk heterojunction devices can be achieved by changing both the diameter of the Ag NSs and the thickness of the Ag NSs buffer layer.

4 Conclusion In order to improve the performance of P3HT:PCBM bulk heterojunction organic solar cells, Ag NSs buffer layers were introduced in between the ITO and the PEDOT:PSS layer. Physical film properties were analyzed using TEM and optical absorption, whilst electronic characteristics were examined using EQE measurements. By incorporating plasmon-active Ag NSs, an enhanced optical absorption and improved J_{sc} is observed. The overall optical absorption of P3HT:PCBM blend films in the spectral range of 350–650 nm are increased ~4% and 6% as a result of utilizing the 20 nm and 40 nm Ag NSs, respectively. The J_{sc} increases from ~3.93 mA/cm^2 to ~4.76 mA/cm^2 and 4.89 mA/cm^2 for 20 nm and 40 nm Ag NSs, respectively. These improvements are due to the light scattering of Ag NSs and the high electric field generated by the excited surface plasmons.

Acknowledgements The authors would like to thank the staff and technicians of Photovoltaic Centre of Excellence, UNSW for their support. We are also grateful to all of our OPV group members for useful discussions and support during this work.

References

[1] M. Campoy-Quiles et al., Nature Mater. **7**, 158 (2008).
[2] M. A. Green et al., Prog. Photovoltaics, Res. Appl. **20**, 12 (2012).
[3] W. Ma et al., Adv. Funct. Mater. **15**, 1617 (2005).
[4] K. Kim et al., Appl. Phys. Lett. **90**, 163511 (2007).
[5] J. Peet et al., Nature Mater. **6**, 497 (2007).
[6] S. H. Park et al., Nature Photon. **3**, 297 (2009).
[7] M.-G. Kang et al., Adv. Mater. **22**, 4378 (2010).
[8] H. A. Atwater et al., Nature Mater. **9**, 205 (2010).
[9] S. S. Kim et al., Appl. Phys. Lett. **93**, 073307 (2008).
[10] D. Fung et al., J. Mater. Chem. **21**, 16349 (2011).
[11] M. Dante et al., J. Phys. Chem. C **112**, 7241 (2008).
[12] L. Qiao et al., Appl. Energy **88**, 848 (2011).
[13] W.-J. Yoon et al., Sol. Energy Mater. Sol. Cells **94**, 128 (2010).
[14] A. J. Morfa et al., Appl. Phys. Lett. **92**, 013504 (2008).